Robust Nonlinear Control of a 6 DOF Parallel Manipulator : Task Space Approach

Hag Seong Kim*
Senior Researcher, Agency for Defense Development, Yuseong P. O. BOX 35-1, Daejon 305-600, Korea
Youngbo Shim
Researcher, Advanced Robotics Research Center, Korea Institute of Science and Technology
Young Man Cho
School of Mechanical and Aerospace Engineering, Seoul National University, Seoul 151-742, Korea
Kyo-Il Lee
School of Mechanical and Aerospace Engineering, Seoul National University

This paper presents a robust nonlinear controller for a 6 degree of freedom (DOF) parallel manipulator in the task space coordinates. The proposed control strategy requires information on orientations and translations in the task space unlike the joint space or link space control scheme. Although a 6 DOF sensor may provide such information in a straightforward manner, its cost calls for a more economical alternative. A novel indirect method based on the readily available length information engages as a potential candidate to replace a 6 DOF sensor. The indirect approach generates the necessary information by solving the forward kinematics and subsequently applying alpha-beta-gamma tracker. With the 6 DOF signals available, a robust nonlinear task space control (RNTC) scheme is proposed based on the Lyapunov redesign method, whose stability is rigorously proved. The performance of the proposed RNTC with the new estimation scheme is evaluated via experiments. First, the results of the estimator are compared with the rate-gyro signals, which indicates excellent agreement. Then, the RNTC with on-line estimated 6 DOF data is shown to achieve excellent control performance to sinusoidal inputs, which is superior to those of a commonly used proportional-plus-integral-plus-derivative controller with a feedforward friction compensation under joint space coordinates and the nonlinear controller under task space coordinates.

Key Words : 6 DOF Manipulator, Robust Nonlinear Task Space Control, Alpha-Beta-Gamma Tracker

1. Introduction

The dynamics and kinematics of a parallel manipulator have been extensively studied by virtue of its high force-to-weight ratio and widespread applications such as vehicle, flight simulator, machine tool, and end-effecter of robot system despite a workspace smaller than a serial robot system (Fichter, 1986 ; Merlet, 2000). Apart from practical engineering reasons, the parallel manipulator has attracted attention in the field of robust nonlinear control theory since it presents a theoretically interesting problem as a typical multi-input-multi-output (MIMO) nonlinear system with uncertainties of inertia, modeling error,

* Corresponding Author,
E-mail : hsfamily@unitel.co.kr
TEL : +82-42-821-3163; **FAX** : +82-42-821-2221
Turret/Mechatronics Team, 1st R&D Center, Agency for Defense Development, Yuseong P. O. BOX 35-1, Daejon 305-600, Korea. (Manuscript **Received** June 5, 2001; **Revised** May 28, 2002)

etc. (Kang et al., 1996 ; Kim et al., 1999, 2000).

The control design for a parallel manipulator typically takes one of two routes: task space control (Kang et al., 1996 ; Lebret et al., 1993 ; Park, 1999 ; Ting et al., 1999) and joint space control (Kim et al. 2000 ; Nguyen et al., 1993) method. The joint space control scheme attempts to track the cylinder lengths pre-computed from the desired 6 DOF trajectories (surge, sway, heave, roll, pitch, and yaw) through inverse kinematics. On the other hand, the task space control implements direct control of the 6 DOF by utilizing the measured or estimated 6 DOF data. Both approaches have attracted much attention in recent years. Kang et al. (1996) and Ting et al. (1999) proved the stability of the task space control system of the Stewart platform driven by a hydraulic servo-system and demonstrate its performance via a simulation study. Kim et al. (1999, 2000) presents a novel nonlinear controller accompanied by stability proofs in the joint space coordinates, under the uncertainties that are too conservative due to the inclusion of gravity and known dynamic characteristics. Park (1999) applied H_∞ robust control strategy based on the linearized model of the Stewart platform. However, it should be noted that an experimental study on the task space control of a 6 DOF parallel manipulator have not been extensively carried out yet.

This paper builds on the previous research efforts by Kang et al. (1996) and Kim et al. (1999, 2000) and proposes a robust nonlinear task space controller (RNTC) based on Lyapunov redesign method to guarantee a practical stability under uncertainties such as inertia, modeling error, and measurement uncertainties like noise, etc. The proposed approach realizes the task space control scheme without a rather costly 6 DOF sensor. Instead, the forward kinematics is solved via the Newton-Raphson method (Dieudonne et al., 1972 ; Nguyen et al., 1993) to obtain 6 DOF information from actuator lengths, and an alpha-beta-gamma tracker is adopted to post-process the acquired 6 DOF information, which results in the noise-filtered velocities and their derivatives (Lewis, 1986 ; Friedland, 1973). The experimental results indeed justify the use of a forward kinematic solution based on the Newton-Raphson method and an alpha-beta-gamma tracker under measurement noise. Finally, the robust nonlinear task space controller with the on-line estimated 6 DOF data is shown to achieve excellent control performance with respect to several sinusoidal inputs, which turns out to be superior to those of the proportional-plus-integral-plus-derivative (PID) controller with a feedforward friction compensation in the joint space coordinates and the nonlinear controller with a feedforward friction compensation (NCFFC) in the task space coordinates.

In Sec. 2, the kinematics and dynamics of a 6 DOF manipulator are briefly presented. Sec. 3 describes the proposed nonlinear control strategy and the accompanying stability analysis. Experimental study is presented in Sec. 4, where the control performance of the proposed task space control (RNTC) approach is compared with those of the PID controller in the joint space coordinates and the NCFFC in the task space coordinates.

2. Dynamic Model of a 6 DOF Parallel Manipulator

The dynamic model of a 6 DOF parallel manipulator is briefly summarized in this paper, since its dynamics and kinematics has been extensively studied (Kim et al., 1999, 2000 ; Lebret et al., 1993 ; Nguyen, 1993 ; Park, 1999). Each coordinate system in Fig. 1 is defined as follows. The { L } coordinate system is the base coordinate system for the inertial frame, while the { U } coordinate system is the moving coordinate system for the body-fixed frame. The linear motions labeled as surge, sway, and heave are along the $x_L - y_L - z_L$ axis. Figure 2 describes the angular motions labeled as roll, pitch, and yaw. Figure 3 shows the definition of each vector required to derive the kinematic and dynamic equations of the parallel mechanism. For detailed description, refer to Kim et al. (1999, 2000) or Park (1999).

With the angular and linear motions of the

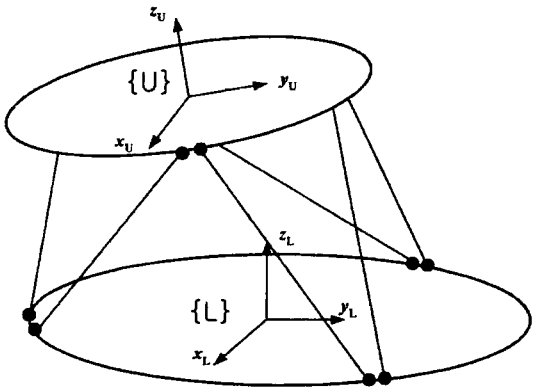

Fig. 1 The Coordinate systems of a 6 DOF parallel manipulator

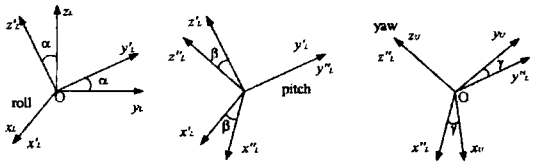

Fig. 2 Rotational transformation from { L } frame to { U } frame without translations

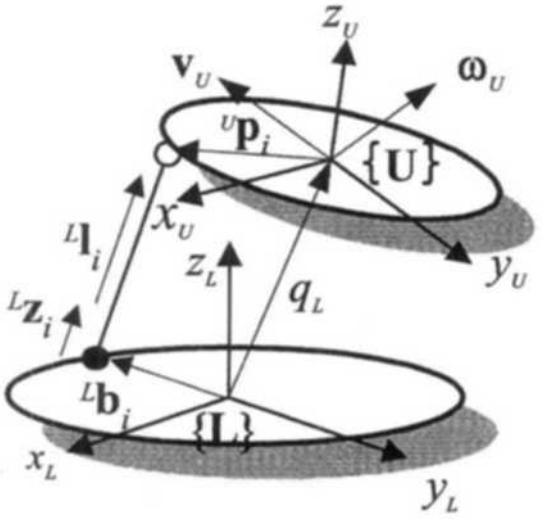

Fig. 3 Definition of the vectors in the kinematic and dynamic equations for a parallel manipulator

parallel manipulator in Fig. 1 and Fig. 2 denoted as α (roll), β (pitch), γ (yaw), x (surge), y (sway), and z (heave), the Euler-Lagrangian method results in the following dynamic equation of motion

$$\mathbf{M}(\mathbf{q}_U, \boldsymbol{\varsigma})\ddot{\mathbf{q}}_U+\mathbf{C}(\mathbf{q}_U, \dot{\mathbf{q}}_U, \boldsymbol{\varsigma})\dot{\mathbf{q}}_U +\mathbf{G}(\mathbf{q}_U, \boldsymbol{\varsigma})=\mathbf{J}^T(\mathbf{q}_U)(\mathbf{f}-\mathbf{f}_f) \quad (1)$$

where $\mathbf{M}(\cdot)\in\mathbf{R}^{6\times6}$ is inertia,
$\mathbf{C}(\cdot)\in\mathbf{R}^{6\times6}$ is Coriolis and centrifugal force,
$\mathbf{G}(\cdot)\in\mathbf{R}^6$ is gravitational force,
$\mathbf{J}(\cdot)\in\mathbf{R}^{6\times6}$ is Jacobian,
$\mathbf{q}_u=[\mathbf{q}_t^T \ \mathbf{q}_a^T]^T\in\mathbf{R}^6$, $\mathbf{q}_t=[x \ y \ z]^T$, and $\mathbf{q}_a=[\alpha \ \beta \ \gamma]^T$,

$\mathbf{f}\in\mathbf{R}^6$ implies the actuator forces, and $\mathbf{f}_f\in\mathbf{R}^6$ is equivalent friction of actuators and joints. It is further assumed that $\dot{\mathbf{M}}-2\mathbf{C}$ in the dynamic equation satisfies the skew symmetric property (Spong et al., 1989). Although the Jacobian is allowed to be singular in a general robot system, it is typical that the parallel manipulator be mechanically designed to avoid such a singularity. Therefore, it does not seem too outrageous to make the following assumptions when realizing a MIMO control strategy.

Assumption 2.1 The Jacobian is not singular.

Assumption 2.2 If $\boldsymbol{\varsigma}$ (constant or time-varying) represents the uncertainties that include inertia, modeling error, and measurement noise, $\boldsymbol{\varsigma}\in\boldsymbol{\Xi}$, where $\boldsymbol{\Xi}$ is compact set.

It is further assumed that the actuator dynamics (both electrical and mechanical) may be neglected in this system except for the friction of each actuator. The actuator friction is explicitly considered as equivalent disturbance force at each joint since it may significantly deteriorate the tracking accuracy.

3. Control Design

The robust nonlinear control theory is a widely known strategy for nonlinear systems with uncertainties to guarantee practical stability (Corless et al, 1981 ; Khalil, 1996 ; and Kim et al, 2000). However, it may not be applied in a straightforward manner to a mechanical system with stick-slip friction that does not satisfy the Caratheodory condition necessary to guarantee the existence and the continuity of the solution, which calls for an additional assumption as described later in this section. Since the details

of definitions (practical stability, uniform ultimate boundedness) and assumptions referred in this paper can be found in Corless et al. (1981) and Khalil (1996), the preliminary materials are presented minimally. Then proposed robust nonlinear task-space control (RNTC) scheme is described in detail.

3.1 Preliminaries

Consider a system

$$\dot{\mathbf{z}}=\mathbf{f}(t, \mathbf{z})+\mathbf{g}(t, \mathbf{z})[\mathbf{u}+\boldsymbol{\delta}(t, \mathbf{z}, \mathbf{u})] \quad (2)$$

where $\mathbf{z}\in\mathbf{R}^n$ is state, $\mathbf{u}=\boldsymbol{\psi}(t, \mathbf{z})+\mathbf{v}\in\mathbf{R}^p$ is control input, and $\boldsymbol{\psi}$, $\mathbf{v}$ are nominal and robust nonlinear controls respectively. The $\mathbf{f}(\cdot)$, $\mathbf{g}(\cdot)$ and $\boldsymbol{\delta}(\cdot)$ are defined in $(t, \mathbf{z}, \mathbf{u})\in[0, \infty)\times\mathbf{D}_r\times\mathbf{R}^p$, where $\mathbf{D}_r=\{\mathbf{z}\in\mathbf{R}^n \,\|\, \|\mathbf{z}\|<r\}$.

Assumption 3.1 The function $\mathbf{f}_i(\cdot)$, $\mathbf{g}_i(\cdot)$ and $\boldsymbol{\delta}_i(\cdot)$ are Caratheodory ones. The solution of the system given by Eq. (2) exists and is absolutely continuous with respect to the initial condition (Corless, 1981).

Remark 3.1 In general, the Caratheodory condition is required for the existence and continuity of the solution. Therefore, it is not straightforward to apply the robust nonlinear control theory to a system with stick-slip, which obviously does not satisfy the Caratheodory condition. On the other hand, it has been shown that if supplement equation and definition can be admissible for a system with friction, there still exists a continuous solution from practical viewpoint (Hahn, 1967 and Radcliffe et al., 1990).

Assumption 3.2 The norm of the uncertain element is bounded by a known function; that is, for all $(t, \mathbf{z})\in\mathbf{R}\times\mathbf{D}_r$

$$\|\boldsymbol{\delta}(t, \mathbf{z}, \mathbf{u})\|\leq\rho(t, \mathbf{z})+k\|\mathbf{v}\|, \qquad 0\leq k<1 \quad (3)$$

where the known function $\rho(\cdot); \mathbf{R}\times\mathbf{R}^n\rightarrow\mathbf{R}_+$ is a Caratheodory function (Khalil, 1996).

3.2 Robust control design

In this subsection, a robust nonlinear controller is synthesized in the task space coordinates on the preliminary materials. The frictions of actuators and joints were converted to equivalent disturbance forces. The following assumptions are further made for robust control design.

Assumption 3.3 There exist positive constant $\overline{M}$, $\underline{M}>0$ such that

$$\underline{M}\mathbf{I}<\mathbf{M}(\mathbf{q}_U, \mathcal{S})<\overline{M}\mathbf{I}, \quad (4)$$

where $\forall\mathbf{q}_U\in\mathbf{D}_r$, $\mathcal{S}\in\boldsymbol{\Xi}$, and $\boldsymbol{\Xi}$ is compact.

Assumption 3.4 It is assumed that each matrix in Eq. (1) can be represented as nominal+deviation:

$$\mathbf{M}(\mathbf{q}_U, \mathcal{S})=\mathbf{M}_0(\mathbf{q}_U, 0)+\delta\mathbf{M}(\mathbf{q}_U, \mathcal{S}),$$
$$\mathbf{C}(\mathbf{q}_U, \dot{\mathbf{q}}_U, \mathcal{S})=\mathbf{C}_0(\mathbf{q}_U, \dot{\mathbf{q}}_U, 0)+\delta\mathbf{C}(\mathbf{q}_U, \dot{\mathbf{q}}_U, \mathcal{S}),$$
$$\mathbf{G}(\mathbf{q}_U, \mathcal{S})=\mathbf{G}_0(\mathbf{q}_U, 0)+\delta\mathbf{G}(\mathbf{q}_U, \mathcal{S}), \text{ and}$$
$$\mathbf{f}_f(\cdot)=\mathbf{f}_{f0}(\cdot)+\delta\mathbf{f}_f(\cdot).$$

Then, the dynamic equation for a tracking error $\tilde{\mathbf{q}}_U=\mathbf{q}_U-\mathbf{q}_{Ud}$ becomes

$$\begin{aligned}\mathbf{M}(\cdot)\ddot{\tilde{\mathbf{q}}}_U+\mathbf{C}(\cdot)\dot{\tilde{\mathbf{q}}}_U=&-\mathbf{M}_0(\cdot)\ddot{\mathbf{q}}_{Ud}-\mathbf{C}_0(\cdot)\dot{\mathbf{q}}_{Ud}\\&-\mathbf{G}_0(\cdot)+\mathbf{J}^T(\cdot)\mathbf{f}\\&-\mathbf{J}^T(\cdot)\mathbf{f}_{f0}+\mathbf{h}_1(\cdot),\end{aligned} \quad (5)$$

where $\mathbf{q}_{Ud}\in\mathbf{R}^6$ is the desired trajectory vector and $\mathbf{h}_1(\cdot)=-\delta\mathbf{M}(\cdot)\ddot{\mathbf{q}}_{Ud}-\delta\mathbf{C}(\cdot)\dot{\mathbf{q}}_{Ud}-\delta\mathbf{G}(\cdot)-\mathbf{J}^T(\cdot)\delta\mathbf{f}_f$.

Kim et al. (1999, 2000) and Kang et al. (1996) lump the gravitational and Coriolis forces into uncertainties for control design since their control scheme is derived for joint space control. As a result, the control performance may be greatly deteriorated by the presence of the large uncertainties. On the other hand, the uncertainities are significantly minimized in the proposed approach by directly compensating for the gravitational force, Coriolis force, etc. as shown in Lemma 3.1.

Lemma 3.1 Suppose that there exists a bounding function $\rho_1(\cdot)$ that satisfies the condition described by Eq. (6). Then, the system given by Eq. (5) is practically stable if the control law described by Eq. (8) is applied with the assumptions 2.1-2.2, 3.1-3.4 and definition given by Eq. (7).

$$\|\boldsymbol{\varphi}_1(\cdot)\|\leq\rho_1(\cdot), \quad (6)$$

where $\boldsymbol{\varphi}_1(\cdot)=\mathbf{h}_1(\cdot)+\delta\mathbf{M}(\cdot)\mathbf{S}_1\dot{\tilde{\mathbf{q}}}_U+\delta\mathbf{C}(\cdot)\mathbf{S}_1\tilde{\mathbf{q}}_U$.

$$\mathbf{e}\equiv[\tilde{\mathbf{q}}_U \quad \dot{\tilde{\mathbf{q}}}_U]^T \quad (7)$$

$$\mathbf{f}=\mathbf{f}_{eq1}+\mathbf{J}^{-t}\mathbf{v}_1,$$

$$\text{and } \mathbf{v}_1=\begin{cases} -\dfrac{\mathbf{w}_1}{\|\mathbf{w}_1\|}\rho_1(\mathbf{e}), & \text{if } \|\mathbf{w}_1\|\geq\varepsilon_1 \\ -\dfrac{\mathbf{w}_1}{\varepsilon_1}\rho_1(\mathbf{e}), & \text{if } \|\mathbf{w}_1\|<\varepsilon_1 \end{cases} \quad (8)$$

$$\begin{aligned}\text{where } \mathbf{f}_{eq1}=\mathbf{J}^{-T}\{&\mathbf{G}_0(\cdot)+\mathbf{M}_0(\ddot{\mathbf{q}}_{Ud}-\mathbf{S}_1\dot{\tilde{\mathbf{q}}}_U)\\&+\mathbf{C}_0(\dot{\mathbf{q}}_{Ud}-\mathbf{S}_1\tilde{\mathbf{q}}_U)-\mathbf{K}_{P1}\tilde{\mathbf{q}}_U \\&-\mathbf{K}_{V1}\dot{\tilde{\mathbf{q}}}_U+\mathbf{J}^T(\cdot)\mathbf{f}_{f0}\},\end{aligned} \quad (9)$$

$\mathbf{K}_{P1}$, $\mathbf{K}_{V1}\in\mathbf{R}^{6\times6}$, $\mathbf{K}_{P1}$, $\mathbf{K}_{V1}$ are symmetric positive definite matrices,

$\mathbf{S}_1=\text{diag}(\mathbf{S}_{1i})\in\mathbf{R}^{6\times6}$, $\mathbf{S}_{1i}>0$,

$\mathbf{K}_{P1}+\mathbf{S}_1\mathbf{K}_{V1}>0$, $\begin{bmatrix}\mathbf{S}_1\mathbf{K}_{P1} & \mathbf{0}\\ \mathbf{0} & \mathbf{K}_{V1}\end{bmatrix}>0$ and

$\mathbf{w}_1(\cdot)=(\dot{\tilde{\mathbf{q}}}_U+\mathbf{S}_1\tilde{\mathbf{q}}_U)\,\rho_1(\cdot)$.

Proof) If Eq. (10) as the Lyapunov function candidate is chosen with control inputs described by Eqs. (8) and (9), the rest of the proof is identical to the one in Kim et al. (1999, 2000).

$$\begin{aligned}V_1=&\frac{1}{2}(\dot{\tilde{\mathbf{q}}}_U+\mathbf{S}_1\tilde{\mathbf{q}}_U)^T\mathbf{M}(\cdot)(\dot{\tilde{\mathbf{q}}}_U+\mathbf{S}_1\tilde{\mathbf{q}}_U)\\&+\frac{1}{2}\tilde{\mathbf{q}}_U{}^T(\mathbf{K}_{P1}+\mathbf{S}_1\mathbf{K}_{V1})\tilde{\mathbf{q}}_U.\end{aligned} \quad (10)$$

Q.E.D.

If the measurements or estimates of 6 DOF data are subject to errors, the control function with the inverse of $\mathbf{J}^T(\cdot)$ is not valid any longer. In this case, the control scheme must be accompanied by other assumptions:

Assumption 3.5 There exist a constant k_1 such that

$$\|\delta\mathbf{J}^T\mathbf{J}_e{}^{-T}\|\leq k_1<1, \quad (11)$$

where $\mathbf{J}_e{}^T(\mathbf{q}'_U, \mathcal{S})=\mathbf{J}^T(\mathbf{q}_U)+\delta\mathbf{J}^T(\delta\mathbf{q}_U, \mathcal{S})$, $\mathbf{q}'_U=\mathbf{q}_U-\delta\mathbf{q}_U$, and $\delta\mathbf{q}_U$ is a uncertainty in the measured or estimated 6 DOF value.

Assumption 3.6 There exist a constant k_2 such that

$$\|\delta\dot{\mathbf{q}}_U+\mathbf{S}_2\delta\mathbf{q}_U\|\leq k_2\|\dot{\tilde{\mathbf{q}}}_U+\mathbf{S}_2\tilde{\mathbf{q}}_U\|,\ 0\leq k_2<1, \quad (12)$$

where $\delta\dot{\mathbf{q}}_U$ is a uncertainty in the measured or estimated 6 DOF velocity.

Remark 3.2 The assumptions 3.5 and 3.6 seem to be conservative and restrictive. If the errors in measurements or estimates of 6 DOF data cannot be bounded, it is impossible to apply the MIMO robust control scheme. Later in Sec. 4.1, the experimental results show that the measurements or the estimates do not violate the assumptions. Furthermore, it is confirmed (not shown in this paper) that even under intentional perturbation of 6 DOF position values by 10% the assumption 3.5 is still satisfied as shown by the kinematic analysis in workspace of the hardware under consideration.

Theorem 3.1 Suppose that the system given by Eq. (5) satisfies the assumptions 2.1-2.2, assumptions 3.1-3.6. In addition, suppose that there exist the bounding functions $\rho_2(\cdot)$ and $\rho_3(\cdot)$ that satisfy the condition given by Eq. (14), and constant k_3 that satisfies the condition given by Eq. (16). Then, the system Eq. (5) is practically stable in the domain $D_r=\{\mathbf{e}\in\mathbf{R}^{12}\,|\,\|\mathbf{e}\|<r\}$ for a given ε_2 with the robust nonlinear control law described by Eq. (15).

$$\begin{aligned}\mathbf{f}_{eq2}=\mathbf{J}_e{}^{-T}\{&\mathbf{G}_0(\cdot)+\mathbf{M}_0(\mathbf{q}'_U)(\ddot{\mathbf{q}}_{Ud}-\mathbf{S}_2\dot{\tilde{\mathbf{q}}}'_U)\\&+\mathbf{C}_0(\mathbf{q}'_U,\dot{\mathbf{q}}'_U)(\dot{\mathbf{q}}_{Ud}-\mathbf{S}_2\tilde{\mathbf{q}}'_U)\\&-\mathbf{K}_{P2}\tilde{\mathbf{q}}'_U-\mathbf{K}_{V2}\dot{\tilde{\mathbf{q}}}'_U+\mathbf{J}_e{}^T(\cdot)\mathbf{f}_{f0}\}\end{aligned} \quad (13)$$

where $\mathbf{K}_{P2}$, $\mathbf{K}_{V2}\in\mathbf{R}^{6\times6}$, $\mathbf{K}_{P2}$, $\mathbf{K}_{V2}$, are symmetric positive definite matrices,

$\mathbf{S}_2=\text{diag}(\mathbf{S}_{2i})\in\mathbf{R}^{6\times6}$, $\mathbf{S}_{2i}>0$, $\mathbf{K}_{P2}+\mathbf{S}_2\mathbf{K}_{V2}>0$,

$\begin{bmatrix}\mathbf{S}_2\mathbf{K}_{P2} & \mathbf{0}\\ \mathbf{0} & \mathbf{K}_{V2}\end{bmatrix}>0$,

$\tilde{\mathbf{q}}_U{}'=\tilde{\mathbf{q}}_U-\delta\mathbf{q}_U$, and $\dot{\tilde{\mathbf{q}}}'_U=\dot{\tilde{\mathbf{q}}}_U-\delta\dot{\mathbf{q}}_U$.

$$\varphi_2(\cdot)=\mathbf{h}_2(\cdot)+\mathbf{h}_3(\cdot)+\mathbf{h}_4(\cdot)-\delta\mathbf{J}^T\mathbf{J}_e{}^{-T}\mathbf{v}_2 \quad (14)$$

$$\begin{aligned}\text{where } \mathbf{h}_2(\cdot)=&-\delta\mathbf{M}(\cdot)\ddot{\mathbf{q}}_{Ud}-\delta\mathbf{C}(\cdot)\dot{\mathbf{q}}_{Ud}\\&-\delta\mathbf{G}(\cdot)-\mathbf{J}_e{}^T(\cdot)\delta\mathbf{f}_f,\\ \mathbf{h}_3(\cdot)=&\delta\mathbf{M}(\cdot)\mathbf{S}_2\dot{\tilde{\mathbf{q}}}_U+\delta\mathbf{C}(\cdot)\mathbf{S}_2\tilde{\mathbf{q}}_U,\\ \mathbf{h}_4(\cdot)=&\mathbf{M}_0\mathbf{S}_2\delta\dot{\mathbf{q}}_U+\mathbf{C}_0\mathbf{S}_2\delta\mathbf{q}_U-\mathbf{K}_{P2}\delta\mathbf{q}_U\\&-\mathbf{K}_{V2}\delta\dot{\mathbf{q}}_U-\delta\mathbf{J}^T\mathbf{f}_{eq2}(\cdot)+\delta\mathbf{J}^T\mathbf{f}_f,\\ \text{and } &\|\mathbf{h}_2(\cdot)+\mathbf{h}_3(\cdot)+\mathbf{h}_4(\cdot)\|\leq\rho_2(\cdot)<\rho_3(\cdot).\end{aligned}$$

$$\mathbf{f}=\mathbf{f}_{eq2}+\mathbf{J}_e{}^{-T}\mathbf{v}_2,$$

$$\text{and } \mathbf{v}_2=\begin{cases} -\dfrac{\rho_3(\mathbf{e})}{1-k_3}\dfrac{\mathbf{w}_2}{\|\mathbf{w}_2\|}, & \text{if } \|\mathbf{w}_2\|\geq\varepsilon_2 \\ -\dfrac{\rho_3(\mathbf{e})}{1-k_3}\dfrac{\mathbf{w}_2}{\varepsilon_2}, & \text{if } \|\mathbf{w}_2\|<\varepsilon_2 \end{cases}, \quad (15)$$

where $\mathbf{w}_2(\cdot)=(\dot{\tilde{\mathbf{q}}}'_U+\mathbf{S}_2\tilde{\mathbf{q}}'_U)\,\rho_3(\cdot)$ and

$$\frac{k_1+2k_2+k_1k_2}{1+k_2}\leq k_3<1. \quad (16)$$

Proof) Choose Eq. (17) as a Lyapunov function candidate.

$$V_2=\frac{1}{2}(\dot{\tilde{\mathbf{q}}}_U+\mathbf{S}_2\tilde{\mathbf{q}}_U)^T\mathbf{M}(\cdot)(\dot{\tilde{\mathbf{q}}}_U+\mathbf{S}_2\tilde{\mathbf{q}}_U)+\frac{1}{2}\tilde{\mathbf{q}}_U^T(\mathbf{K}_{P2}+\mathbf{S}_2\mathbf{K}_{V2})\tilde{\mathbf{q}}_U \quad (17)$$

The positive definite and decrescent property of this candidate function was shown with assumption 3.3 in Kang et al. (1996). As a result, there exist constants γ_1, $\gamma_2>0$ such that $\gamma_1\|\mathbf{e}\|^2\le V_2\le\gamma_2\|\mathbf{e}\|^2$ for Eq. (17).

Under the assumption 3.4 with additional measurement or estimation error, the system Eq. (1) can be recast into

$$\mathbf{M}(\cdot)\ddot{\tilde{\mathbf{q}}}_U+\mathbf{C}(\cdot)\dot{\tilde{\mathbf{q}}}_U=-\mathbf{M}_0\ddot{\mathbf{q}}_{Ud}-\mathbf{C}_0\dot{\mathbf{q}}_{Ud}-\mathbf{G}_0+\mathbf{J}_e^T\mathbf{f}-\mathbf{J}_e^T\mathbf{f}_{f0}-\delta\mathbf{J}^T\mathbf{f}+\delta\mathbf{J}^T\mathbf{f}_f+\mathbf{h}_2(\cdot). \quad (18)$$

Then, with the assumption 2.1, 3.1-3.3, the skew symmetric property of $\dot{\mathbf{M}}-2\mathbf{C}$, and control input described by Eq. (15) that compensates the uncertainties, the derivative of the Lyapunov candidate function becomes

$$\dot{V}_2\le-\gamma_3\|\mathbf{e}\|^2+(\dot{\tilde{\mathbf{q}}}'_U+\mathbf{S}_2\tilde{\mathbf{q}}'_U)^T\mathbf{v}_2+(1+k_2)\|\dot{\tilde{\mathbf{q}}}'_U+\mathbf{S}_2\tilde{\mathbf{q}}'_U\|\rho_2+(k_1+k_1k_2+k_2)\|\dot{\tilde{\mathbf{q}}}'_U+\mathbf{S}_2\tilde{\mathbf{q}}'_U\|\cdot\|\mathbf{v}_2\|, \quad (19)$$

where $\gamma_3=\lambda_{\min}\left[\begin{bmatrix}\mathbf{S}_2\mathbf{K}_{P2} & \mathbf{0}\\ \mathbf{0} & \mathbf{K}_{V2}\end{bmatrix}\right]$.

In the case $\|\mathbf{w}_2\|\ge\varepsilon_2$, Eq. (19) can be further developed using Eq. (15) and Eq. (16).

$$\begin{aligned}\dot{V}_2&\le-\gamma_3\|\mathbf{e}\|^2+(\dot{\tilde{\mathbf{q}}}'_U-\mathbf{S}_2\tilde{\mathbf{q}}'_U)^T\mathbf{v}_2+(1+k_2)\|\mathbf{w}_2\|+\frac{k_1+k_1k_2+k_2}{1-k_3}\|\mathbf{w}_2\|\\&=-\gamma_3\|\mathbf{e}\|^2+\frac{k_1+k_1k_2+k_2+(1+k_2)(1-k_3)}{1-k_3}\|\mathbf{w}_2\|-\frac{1}{1-k_3}\|\mathbf{w}_2\| \quad (20)\\&=-\gamma_3\|\mathbf{e}\|^2+\frac{k_1+k_1k_2+2k_2-k_3(1+k_2)}{1-k_3}\|\mathbf{w}_2\|\le-\gamma_3\|\mathbf{e}\|^2\end{aligned}$$

In the case $\|\mathbf{w}_2\|<\varepsilon_2$, Eq. (19) can be reduced to

$$\begin{aligned}\dot{V}_2&\le-\gamma_3\|\mathbf{e}\|^2+(1+k_2)\|\mathbf{w}_2\|+\frac{(k_1+k_1k_2+k_2-1)}{\varepsilon_2(1-k_3)}\|\mathbf{w}_2\|^2\\&\le-\gamma_3\|\mathbf{e}\|^2+(1+k_2)\left\{\|\mathbf{w}_2\|-\frac{(1-k_1-k_1k_2-k_2)}{\varepsilon_2(1-k_3)(1+k_2)}\|\mathbf{w}_2\|^2\right\} \quad (21)\\&<-\gamma_3\|\mathbf{e}\|^2+2\left\{\|\mathbf{w}_2\|-\frac{1}{\varepsilon_2}\|\mathbf{w}_2\|^2\right\}\le-\gamma_3\|\mathbf{e}\|^2+\frac{\varepsilon_2}{2}.\end{aligned}$$

Subsequently, ε_2 and $\mu(\varepsilon_2)$ are chosen such that $\varepsilon_2<2\gamma_3\cdot\gamma_2^{-1}\cdot\gamma_1\cdot r^2$ and $\mu(\varepsilon_2)=\sqrt{\gamma_3^{-1}(\varepsilon_2/2)+h}$ for $h>0$,

$$\dot{V}_2\le-\gamma_3\|\mathbf{e}\|^2+\frac{\varepsilon_2}{2}<0,\ \forall\mu(\varepsilon)\le\|\mathbf{e}\|<r. \quad (22)$$

Therefore, for any given ε_2, if $\mu(\varepsilon_2)<\|\mathbf{e}(t_0)\|<\gamma_2^{-1}(\gamma_1(r))$, then $\dot{V}_2$ is strictly negative, which implies that there exists a finite time t_1 such that

$$t_1\le t_0+\frac{1}{\gamma_3 h}\left\{\gamma_2\|\mathbf{e}(t_0)\|^2-\gamma_1\left(\frac{\varepsilon_2}{2\gamma_3}+h\right)\right\},$$

and the state stays in the set $B_r=\{\mathbf{e}:\|\mathbf{e}\|\le\mu(\varepsilon_2)\}$ after time t_1 (Canudas et al., 1996). Consequently, the system response is uniformly ultimately bounded via the controller described by Eq. (15), which implies practical stability. Q.E.D.

4. Experimental Results

In this section, the performance of the proposed RNTC is investigated with a 6 DOF-manipulator in Fig. 4 via experiments. The parallel mechanism consists of six electrical cylinders (ETS32-B08PZ20-CMA150-A, Parker Inc.). The control law is implemented with a Pentium III 800 PC-based system that includes motor amplifiers (OEM-570T, Compumotor Inc.), the D/A board for actuators (AT-A0-6/10, NI Corp.), the encoder board (AT6450, Parker Inc.), the 12bit A/D and D/A converter (LAB-PC+, NI Corp.) for the rate transducer (RT02-0820-1, Humphrey Inc.). The sampling time for the control system is 3 msec. The parameters of the parallel manipulator are summarized in Table 1.

Only the length of each cylinder can be readily

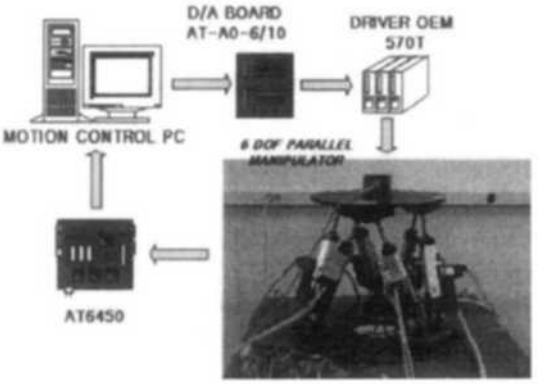

Fig. 4 Control system for a 6 DOF parallel manipulator

Table 1 Parameters of a 6 DOF parallel manipulator

Parameter	Description	Nominal value	Unit
l_{min}, l_{max}	Minimum/Maximum Stroke of Cylinder	0.365/0.51	m
m	Mass of Upper Plate	24.0	Kg
I_{xx}, I_{yy}, I_{zz}	Moment of Inertia of Upper Plate	0.4315, 0.4316, 0.6111	$Kg \cdot m^2$
R_L, R_U	Radius of Lower Plate/Upper Plate	0.24, 0.16	m

measured in this system. Although the rate transducer is employed in the experimental study, its use is limited to validation when the fidelity of angular motion estimates is examined. Therefore, the control law described by Eq. (15) may not be directly applied in the task space coordinates. This apparent cul-de-sac is circumvented by developing an indirect estimation methodology. First, the Newton-Raphson method is applied to acquire the forward kinematic solutions from the actuator lengths. The performance of the Newton-Raphson method is excellent with a proper choice of the initial condition (Dieudonn et al., 1972). An observer (Kang et al., 1998) or estimator (Jung et al., 1994) was considered as an alternative but was quickly discarded since the high gain may result in so-called "peaking phenomenon", which may allow the estimates to deviate for a short period of time despite good overall convergence. Therefore the numerical approach is adopted in this paper to produce more stable estimates with well-selected initial conditions. An alpha-beta-gamma tracker further processes the estimates to generate 6 DOF velocities and accelerations. The direct derivatives of 6 DOF signals from instantaneous velocities of the actuators and Jacobian may be subject to large error due to the measurement noise. The sensing and estimation procedure is enumerated as follows :

1) Measure the length of each cylinder.

2) Use the alpah-beta-gamma tracker for each length signal.

3) Apply the numerical method to obtain a forward kinematic solution

4) Use the alpah-beta-gamma tracker to acquire the velocity and acceleration of each 6 DOF position.

5) Compute the control inputs with the estimates.

Equipped with the estimation methodology, experimental results are presented.

4.1 Estimation of the 6 DOF information

In this subsection, the performance of the numerical method and the alpha-beta-gamma tracker are examined with noisy measurements, which is necessary since the resulting estimates determines the control inputs to compensate the nonlinear terms and uncertainties. First, the inverse kinematic solutions based on the 6 DOF estimates from the numerical method (tolerance : 10^{-7}) and the tracker are compared to measured displacements in an effort to verify the performance of the above estimation method. Figure 5 shows less than 0.1% errors (normal length 435 mm) under a given moving condition (roll (2.0 deg/ 1.0 Hz), pitch (5.0 deg/0.5 Hz), yaw (2.5 deg/ 1.0 Hz) and heave (5.0 mm/0.5 Hz) motion), which implies that the uncertainties of position errors or Jacobian are negligible and assumption 3.5 is satisfied. Second, the rate transducer (RT 02-0820-1, Humphrey Inc.) is installed to provide a foundation for the comparison between the estimated and measured rotational velocities of three angular motions. Figure 6 presents the comparison between the rate transducer reading and the estimated angular velocity under a sinusoidal roll motion (5.0 degree and 0.5 Hz), which suggests that the estimation scheme can produce the derivatives of motion signals without complicated calculation on the kinematic relation. It should be noted that the unavailability of the corresponding sensors does not allow the same type of comparison to be made along the translational direction. Still, the proposed approach can be extended to produce accurate estimates of the linear motions.

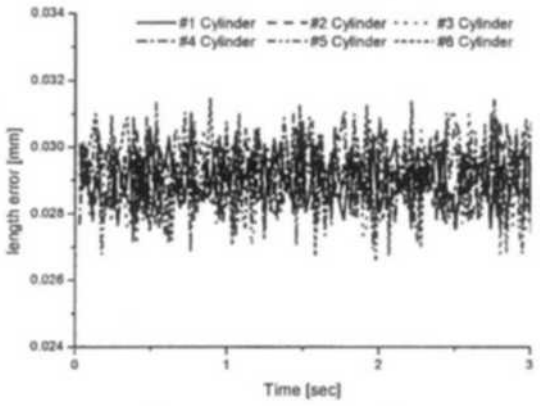

Fig. 5 Errors between measured lengths and inverse kinematic solutions from the estimated 6 DOF data based on the numerical method

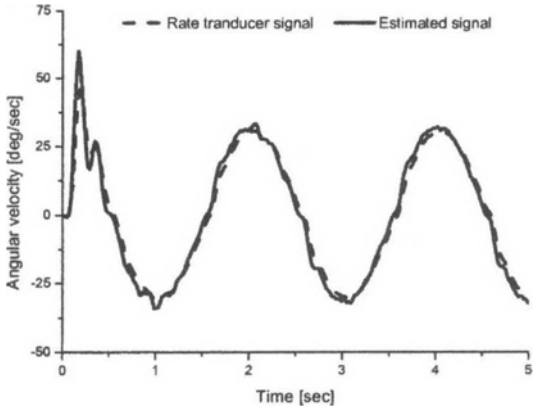

Fig. 6 Comparison between the measured and the estimated signals by the tracker under a roll motion (5.0 deg /0.5 Hz)

4.2 Control performance

This subsection presents the performance of the proposed robust nonlinear task space control (RNTC) strategy with the estimates of 6 DOF signals obtained in the previous subsection. The feedforward friction compensation in the equivalent control input utilizes the friction characteristics (Coulomb and viscous frictions) of each actuator, which have been previously shown in Park (1999) (The Coulomb and viscous friction are in the ranges ; 32～88 N and 478～778 N/(m/sec), respectively. The scale factor is 267 N/volt).

A proportional-plus-integral-plus-derivative controller with feedforward friction compensation (PIDFFC) and the nonlinear controller with

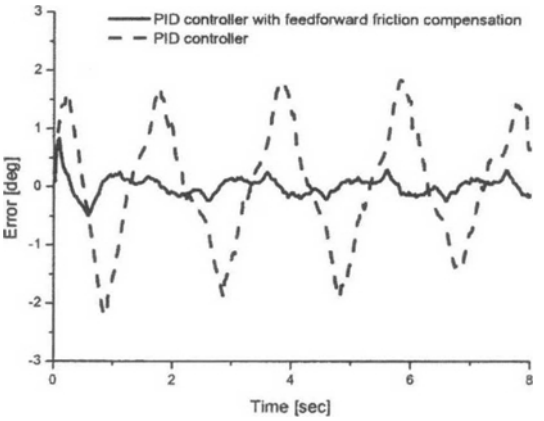

Fig. 7 Comparison between the PIDFFC and the PID only under a roll motion (5.0 deg/0.5 Hz)

feedforward friction compensation (NCFFC ; Eq. (13)) are also applied primarily to provide a benchmark. It should be noted that the PID control scheme could be a practically attractive alternative by virtue of the simple structure and easy implementation. However, the performance of the PID control without friction compensation degrades drastically in the system under consideration as shown in Fig. 7. Therefore, the PID control strategy with feedforward friction compensation (PIDFFC) is implemented in order to compare the PID control scheme and the robust nonlinear control scheme or a fair basis.

The PIDFFC gains K_{P_gain}, K_{I_gain}, K_{D_gain} are tuned to be 100, 800, and 20, respectively. The control gains for the RNTC and the NCFFC are :

$$\mathbf{K}_{P2}=1\times10^{5}\cdot\begin{bmatrix} 0.304 & 0 & 0 & 0 & 0.0156 & 0 \\ 0 & 0.304 & 0 & -0.0094 & 0 & 0 \\ 0 & 0 & 2.5 & 0 & 0 & 0 \\ 0 & -0.0094 & 0 & 0.0208 & 0 & 0 \\ 0.0156 & 0 & 0 & 0 & 0.0347 & 0 \\ 0 & 0 & 0 & 0 & 0 & 0.0139 \end{bmatrix},$$

$$\mathbf{K}_{V2}=1\times10^{4}\cdot\begin{bmatrix} 0.135 & 0 & 0 & 0 & 0.009 & 0 \\ 0 & 0.27 & 0 & -0.009 & 0 & 0 \\ 0 & 0 & 2.03 & 0 & 0 & 0 \\ 0 & -0.009 & 0 & 0.02 & 0 & 0 \\ 0.009 & 0 & 0 & 0 & 0.02 & 0 \\ 0 & 0 & 0 & 0 & 0 & 0.0027 \end{bmatrix},$$

$$S_2=\begin{bmatrix} 10.0 & 0 & 0 & 0 & 0 & 0 \\ 0 & 10.0 & 0 & 0 & 0 & 0 \\ 0 & 0 & 10.0 & 0 & 0 & 0 \\ 0 & 0 & 0 & 10.0 & 0 & 0 \\ 0 & 0 & 0 & 0 & 10.0 & 0 \\ 0 & 0 & 0 & 0 & 0 & 10.0 \end{bmatrix}, \text{ and } \varepsilon_2=0.5.$$

The initial values of the control gains are based on the PID gains through the kinematic relation between the joint space coordinates and the task space coordinates. Then, the initial proportional and derivative gain matrices for the RNTC or the NCFFC are tuned by experimental trade-off.

It is easy to check that the matrices satisfy the positive definiteness condition in Lemma 3.1 and Theorem 3.1. Although the RNTC and the NCFFC gains seem much higher than those of PIDFFC, they are not actually, in that the control forces of the RNTC are calculated on-line from the gain matrices and Jacobian.

Figures 8~10 show that the RNTC has superior overall tracking performance for a given roll motion (5 deg/0.5 Hz) than the PIDFFC and the NCFFC despite slightly worse performance along the command direction. This seemingly unexpected behavior can be explained by noting that the RNTC and the NCFFC aims to control along all directions in the task space, while the PIDFFC simply tracks the desired lengths along a given direction. In other words, the PIDFFC does not take into account the sensitivity of 6 DOF displacements on length variation, that is, Jacobian.

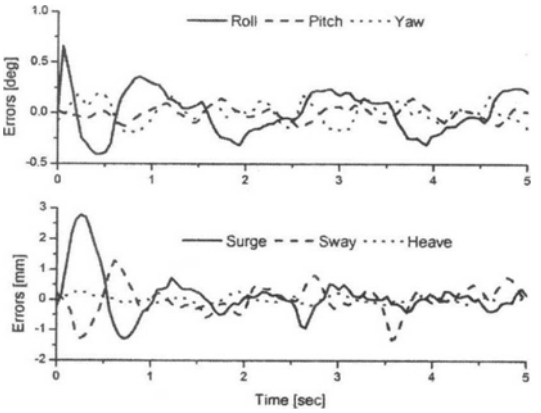

Fig. 8 6 DOF motion errors through the PIDFFC under a roll motion (5.0 deg/0.5 Hz)

Therefore, the actuator may cause the relatively large undesired motions along other directions with negligible effect on the main motion. It should also be noted that the integral action in PIDFFC decreases the length errors in a low velocity range by virtue of its effectiveness under the friction environment. However, the proposed RNTC and the NCFFC based on the proportional-plus-derivative control fails to derive the errors to zero because the feedforward friction compensation does not perform well due to stick-slip property even though the friction uncertainty is explicitly considered during control design. In general, the overestimated uncertainty during control design result in larger control gains which may cause undesirable chattering. The above discussion motivates the development of more

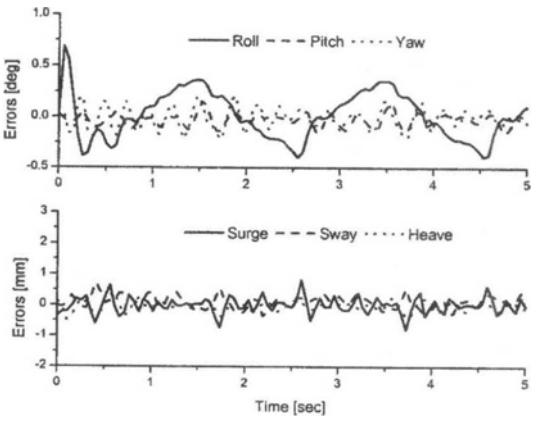

Fig. 9 6 DOF motion errors through the NCFFC under a roll motion (5.0 deg/0.5 Hz)

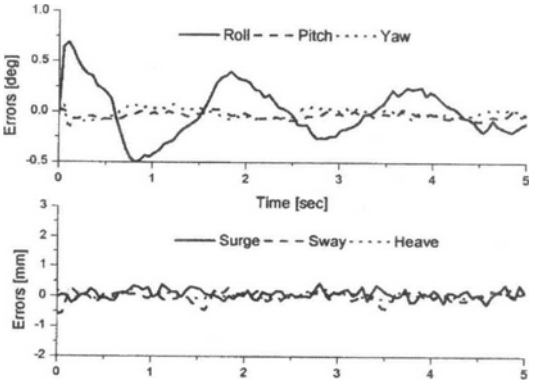

Fig. 10 6 DOF motion errors through the RNTC under a roll motion (5.0 deg/0.5 Hz)

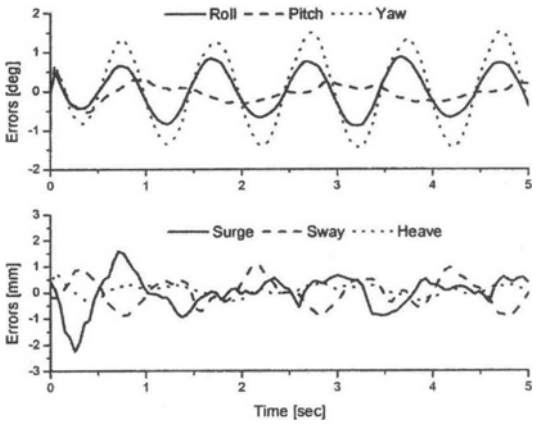

Fig. 11 6 DOF motion errors through the PIDFFC under roll (2.0 deg/1.0 Hz), pitch (5.0 deg/0.5 Hz), yaw (2.5 deg/1.0 Hz) and heave (5.0 mm/0.5 Hz) motions

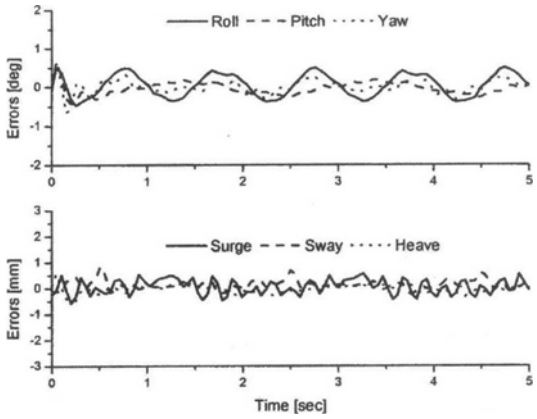

Fig. 12 6 DOF motion errors through the proposed NCFFC under roll (2.0 deg/1.0 Hz), pitch (5.0 deg/0.5 Hz), yaw (2.5 deg/1.0 Hz) and heave (5.0 mm/0.5 Hz) motions

refined control strategy to minimize the effect of dry friction, which is the topic of future research.

Figures 11~13 show tracking errors under the sinusoidal inputs along four directions ; roll (2.0 deg/1.0 Hz), pitch (5.0 deg/0.5 Hz), yaw (2.5 deg/1.0 Hz) and heave (5.0 mm/0.5 Hz) motion. In contrast to one directional command, the RNTC shows tracking performance superior to those of the NCFFC and the PIDFFC along all 6 DOF directions. The RNTC's superior performance stems from its task space based design, cancellation of nonlinearities: the inertia force

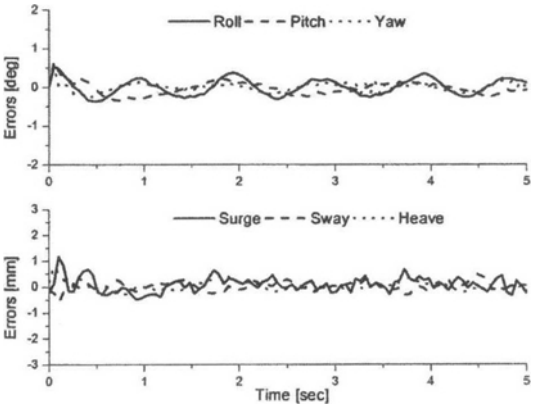

Fig. 13 6 DOF motion errors through the proposed RNTC under roll (2.0 deg/1.0 Hz), pitch (5.0 deg/0.5 Hz), yaw (2.5 deg/1.0 Hz) and heave (5.0 mm/0.5 Hz) motions

for a given acceleration, the gravitational force, the Coriolis and centrifugal forces in Eq. (13), and the consideration on the system uncertainties (modeling errors, frictions, etc). The maximum translational error of the RNTC is smaller than ± 0.4 mm, while those of the PIDFFC and the NCFFC are larger than ± 1.0 mm and ± 0.5 mm, respectively. The maximum rotational error of the RNTC falls below ± 0.3 deg, while those of the PIDFFC and the NCFFC exceed ± 1.5 deg and ± 0.4 edg, repectively. Overall the RNTC outperforms the PIDFFC and the NCFFC under the input with multi-directional high frequency components.

5. Conclusions

A robust nonlinear task space control strategy based on the Lyapunov redesign methodology is proposed and implemented for a 6 DOF parallel manipulator. The Newton-Raphson method and the alpha-beta-gamma filtering algorithm are employed in order to realize the proposed control scheme without direct measurements of 6 DOF information. The former helps to solve the instantaneous forward kinematic equations and the latter provides a simple route to state estimates without an explicit plant model. The experimental results under several sinusoidal commands show that the RNTC has excellent tracking perfor-

mance under nonlinearity and parameter uncertainties that are not taken into consideration in the dynamic model of the parallel manipulator. Moreover, the task space control strategy is shown to outperform the SISO control scheme under severe nonlinearity, which implies its viability in a real-world application.

Acknowledgement

This research was supported by a grant from the BK-21 Program for Mechanical and Aerospace Engineering Research at Seoul National University, the Micro Thermal System Research Center through the Korea Science and Engineering Foundation, and the National Research Center on Innovative Parallel Mechanism Platforms.

References

Canudus de Wit, C., Siciliano, B., and Bastin, G. 1996, *Theory of Robot Control*, Springer-Verlag.

Corless, M. J. and Leitmann, G., 1981, "Continuous State Feedback Guaranteeing Uniform Ultimate Boundedness for Uncertain Dynamic Systems," *IEEE Transactions on Automatic Control*, Vol. 26, pp. 153~158.

Dieudonne, J. E., Parrish, R. V. and Bardusch, R. E., 1972, "An Actuator Extension Transformation for a Motion Simulator and an Inverse Transformation applying Newton-Raphson Method," *NASA Technical Report* D-7067.

Fichter, E. F., 1986, "A Stewart Platform-Based Manipulator : General Theory and Practical Construction," *The International Journal of Robotics Research*, Vol. 5, No. 2, pp. 157~182.

Friedland, B., 1973, "Optimum Steady-State Position and Velocity Estimation Using Sampled Position data," *IEEE Transactions on Aerospace and Electronic Systems*, Vol. AES-9, No. 6, pp. 906~911.

Hahn, W., 1967, *Stability of Motion*, Springer-Verlag, New York.

Jung, G. H. and Lee, K. -I, 1994, "Real-time Estimation of Stewart Platform Forward Kinematic Solution," *Transactions of the KSME*, Vol. 18, No. 7, pp. 1632~1642.

Kang, J. -Y., Kim, D. H., and Lee, K. -I, 1996, "Robust Tracking Control of Stewart Platform," *Proceedings of the 35th Conference of Decision and Control*, Kobe, Japan, pp. 3014~3019.

Kang, J. -Y., Kim, D. H. and Lee, K. -I, 1998, "Robust Estimator Design for Forward Kinematics Solution of a Stewart Platform," Journal of Robotic Systems, Vol. 15, pp. 30~42.

Khalil, H. K., 1996, *Nonlinear Systems*, Prentice-Hall, Englewood Cliffs, New Jersey.

Kim, D. H., Kang, J. -Y. and Lee, K. -I., 1999, "Nonlinear Robust Control Design for a 6 DOF Parallel Robot," *KSME International Journal*, Vol. 13, No. 7, pp. 557~568.

Kim, D. H., Kang, J. -Y. and Lee, K. -I., 2000, "Robust Tracking Control Design for a 6 DOF Parallel Manipulator," *Journal of Robotic Systems*, Vol. 17, pp. 527~547.

Lebret, G., Liu, K.' and Lewis, F. L., 1993, "Dynamic Analysis and Control of a Stewart Platform Manipulator," *Journal of Robotic Systems*, Vol. 10, No. 5, pp. 629~655.

Lewis, F., 1986, *Optimal Estimation with an Introduction to Stochastic Control Theory*, John Wiley and Sons, Inc., USA.

Merlet, J. P., 2000, *Parallel Robots*, Kluwer Academic Publisher, Netherlands.

Nguyen, C. C., Antrazi, S., Zhou, Z. -L. and Campbell, C., 1993, "Adaptive Control of a Stewart Platform-Based Manipulator," *Journal of Robotic Systems*, Vol. 10, No. 5, pp. 657~687.

Park, C. G., 1999, "Analysis of Dynamics including Leg Inertia and Robust Controller Design for a Stewart Platform," Ph. D. thesis, Seoul National University.

Radcliffe, C. J. and Southward, S. C., 1990, "A Property of Stick-Slip Friction Models which Promotes Limit Cycle Generation," *Proceedings on American Control Conference*, San Diego, CA, pp. 1198~1203.

Spong, M. W. and Vidyasagar, M., 1989, *Robot Dynamics and Control*, John Wiley & Sons, Inc.

Ting, Y., Chen, Y. -S. and Wang, S. -M., 1999, "Task-space Control Algorithm for Stewart Platform," *Proceedings of the 38th Conference* on Decision and Control, Phoenix, Arizona, pp. 3857~3862.